



Published in final edited form as:

*Nat Biotechnol.* 2014 September ; 32(9): 915–925. doi:10.1038/nbt.2972.

## Multi-platform and cross-methodological reproducibility of transcriptome profiling by RNA-seq in the ABRF Next-Generation Sequencing Study

Sheng Li<sup>#1,2</sup>, Scott W. Tighe<sup>#3</sup>, Charles M. Nicolet<sup>4</sup>, Deborah Grove<sup>5</sup>, Shawn Levy<sup>6</sup>, William Farmerie<sup>7</sup>, Agnes Viale<sup>8</sup>, Chris Wright<sup>9</sup>, Peter A. Schweitzer<sup>10</sup>, Yuan Gao<sup>11</sup>, Dewey Kim<sup>11</sup>, Joe Boland<sup>12</sup>, Belynda Hicks<sup>12</sup>, Ryan Kim<sup>13</sup>, Sagar Chhangawala<sup>1,2</sup>, Nadereh Jafari<sup>14</sup>, Nalini Raghavachari<sup>15</sup>, Jorge Gandara<sup>1,2</sup>, Natàlia Garcia-Reyero<sup>16</sup>, Cynthia Hendrickson<sup>6</sup>, David Roberson<sup>12</sup>, Jeffrey Rosenfeld<sup>17</sup>, Todd Smith<sup>18</sup>, Jason G. Underwood<sup>19</sup>, May Wang<sup>20</sup>, Paul Zumbo<sup>1,2</sup>, Don A. Baldwin<sup>21,+</sup>, George S. Grills<sup>10,+</sup>, and Christopher E. Mason<sup>1,2,+</sup>

<sup>1</sup>Department of Physiology and Biophysics, Weill Cornell Medical College, New York, New York, USA

<sup>2</sup>The HRH Prince Alwaleed Bin Talal Bin Abdulaziz Alsaud Institute for Computational Biomedicine, Weill Cornell Medical College, New York, New York, USA

<sup>3</sup>Vermont Cancer Center, University of Vermont, Burlington, Vermont, USA

<sup>4</sup>Keck School of Medicine, University of Southern California, Los Angeles, California, USA

<sup>5</sup>The Huck Institutes of the Life Sciences, Pennsylvania State University, University Park, Pennsylvania, USA

<sup>6</sup>HudsonAlpha Institute for Biotechnology, Huntsville, Alabama, USA

<sup>7</sup>Interdisciplinary Center for Biotechnology Research, University of Florida, Gainesville, Florida, USA

<sup>8</sup>Memorial Sloan-Kettering Cancer Institute, New York, New York, USA

<sup>9</sup>Roy J. Carver Biotechnology Center, University of Illinois, Urbana, Illinois, USA

<sup>10</sup>Biotechnology Resource Center, Institute of Biotechnology, Cornell University, Ithaca, New York, USA

<sup>11</sup>Department of Biomedical Engineering, Johns Hopkins University, Baltimore, Maryland, USA

<sup>12</sup>NIH/NCI/SAIC-Frederick, Gaithersburg, Maryland, USA

<sup>13</sup>Genome Center, University of California, Davis, Davis, California, USA

<sup>14</sup>Center for Genetic Medicine, Northwestern University, Chicago, Illinois, USA

<sup>15</sup>NIH/NHLBI, Bethesda, Maryland, USA

<sup>#</sup>Corresponding authors Correspondence should be sent to D.A.B. (pathonomics@gmail.com), G.S.G. (gsg34@cornell.edu) or C.E.M. (chm2042@med.cornell.edu).

**Competing Financial Interests** The authors declare that they have no relevant competing financial interests.

<sup>16</sup>Institute for Genomics, Biocomputing and Biotechnology, Mississippi State University, Starkville, Mississippi, USA

<sup>17</sup>Division of High Performance and Research Computing, University of Medicine and Dentistry of New Jersey, Newark, New Jersey, USA

<sup>18</sup>PerkinElmer Inc., Seattle, Washington, USA

<sup>19</sup>University of Washington, Department of Genome Sciences. Seattle, Washington, USA

<sup>20</sup>Department of Biomedical Engineering, Georgia Institute of Technology and Emory University, Atlanta, Georgia, USA

<sup>21</sup>Pathonomics LLC, Philadelphia, Pennsylvania, USA

# These authors contributed equally to this work.

## Abstract

High-throughput RNA sequencing (RNA-seq) dramatically expands the potential for novel genomics discoveries, but the wide variety of platforms, protocols and performance has created the need for comprehensive reference data. Here we describe the Association of Biomolecular Resource Facilities next-generation sequencing (ABRF-NGS) study on RNA-seq. We tested replicate experiments across 15 laboratory sites using reference RNA standards to test four protocols (polyA-selected, ribo-depleted, size-selected and degraded) on five sequencing platforms (Illumina HiSeq, Life Technologies' PGM and Proton, Pacific Biosciences RS and Roche's 454). The results show high intra-platform and inter-platform concordance for expression measures across the deep-count platforms, but highly variable efficiency and cost for splice junction and variant detection between all platforms. These data also demonstrate that ribosomal RNA depletion can both enable effective analysis of degraded RNA samples and be readily compared to polyA-enriched fractions. This study provides a broad foundation for cross-platform standardization, evaluation and improvement of RNA-seq.

## Introduction

RNA-seq is an important analytical technique that leverages the capacity of high-throughput sequencing instruments to quantitatively sample a population of RNA molecules with a large number of "reads" or parallel reactions on discrete templates<sup>1,2</sup>. Depending on experimental goals, sample types and read depths, results from RNA-seq data can be similar or superior to those from microarray data<sup>3-5</sup>. However, each sequencing platform has unique aspects of library synthesis, sequencing, alignment, and data processing<sup>6-9</sup>. Thus, many questions remain about RNA-seq in regards to inter-operability between platforms, cross-site reproducibility, bioinformatics methods and the sources of variance in results with both existing and emerging protocols, such as those for degraded RNA.

Notably, prior work comparing microarray platforms and methods showed high levels of inter-platform concordance for the ability to detect differentially expressed genes. The Microarray Quality Control (MAQC) Consortium landmark study<sup>10</sup> examined the degree of variance within and across many different microarray platforms and found similar

coefficients of variation between platforms. The MAQC data also provided an important benchmark for the application of microarray technologies to clinical assays. For high-throughput sequencing platforms, however, very little data exist about cross-site variation of expression measures. Only two inter-site variation studies are publicly available: the MAQC-III (a.k.a. the Sequencing Quality Control Consortium, SEQC)<sup>11</sup> study and the GEUVARDIS Consortium<sup>12</sup>. These studies were either limited to one platform or did not assess some newer RNA-seq methods that are now widely used. Moreover, important RNA profiling parameters such as differential expression and splice variant detection have not been consistently evaluated. Thus, these studies do not answer key questions about the degree of concordance for RNA-seq across platforms and methods and also about the read depth, type, and length of sequence reads required to fully characterize a sample with current techniques<sup>13-16</sup>. Moreover, RNA-seq is an extremely useful method for exploring the expression of sequence variants, detecting novel RNAs and for discriminating between transcript splicing isoforms<sup>17-20</sup>, but there is no “gold standard” of reference data on the dynamic range of differential expression and splicing that includes different sample preparation protocols, instruments and data analysis strategies.

To address this challenge, members of the Association of Biomolecular Resource Facilities (ABRF)<sup>21</sup> designed and conducted the first phase of a large-scale ABRF-NGS Study with a focus on RNA-seq. The goals of the ABRF-NGS Study are to evaluate the performance of NGS platforms and to identify optimal methods and best practices. A wide range of variables was evaluated, including library preparation methods (polyA-enriched and ribo-depleted), size-specific fractionation (1, 2 and 3 kb) and RNA integrity (using heat, RNase A and sonication to degrade the RNA). The latter variable was chosen to mimic some of the damaging effects of tissue fixation with formalin, which is a well-recognized issue for RNA profiling of formalin-fixed, paraffin-embedded (FFPE) clinical specimens<sup>22-24</sup>. Finally, we leveraged a data set of 18,124 PrimePCR reactions and used it with 802 previously published<sup>10</sup> TaqMan RT-qPCR reactions as orthogonal measurements to gauge the linear response and dynamic range of the RNA-seq results from the different platforms and protocols. Both platform-agnostic and platform-specific aligners were also compared to support the validity of the conclusions. Taken together, these data represent a broad cross-platform characterization of widely used RNA standards and to our knowledge provide the largest comprehensive comparison of results from degraded, full-length and size-selected RNA across sequencing platforms and protocols.

## Results

### Platforms, RNA samples and sequencing protocols

Although comparisons of high-throughput sequencing platforms and sample preparation protocols have been reported in past studies<sup>6,5-27</sup>, no other study has been conducted using five platforms and two standardized RNA samples replicated at multiple sites (Fig. 1). Platforms evaluated included the Illumina HiSeq 2000/2500, Roche 454 GS FLX+, Life Technologies Ion Personal Genome Machine (PGM) and Proton, and the Pacific Biosciences RS (PacBio)<sup>6, 8, 28</sup>. Data were generated and analyzed by the members of five ABRF Research Groups, including 25 core facilities at 20 different institutions (Fig. 1 and

Supplementary Table 1). Additional data from an Illumina MiSeq v2 instrument were used to compare metrics derived from different read lengths from the same Illumina library preparation and sequencing methods. Detection of differential RNA abundance was evaluated using two commercially available and very distinct RNA samples: A = RNA from cancer cell lines; B = RNA from pooled normal human brain tissues; and two pre-defined mixtures of these samples (C = [75% A + 25% B]; D = [25% A + 75% B]). All standardized RNA samples also contained synthetic RNA spike-ins from the External RNA Control Consortium (ERCC)<sup>10, 29, 30</sup>. Results from high-quality RNA on the Illumina HiSeq 2500 platform were compared to results on the same platform from RNAs degraded using three degradation conditions: heat, RNase and sonication. The RNA reference samples were degraded to a RIN (RNA integrity number) of 2 or less. In addition, results from ribosomal RNA-depleted and polyA-enriched libraries from intact RNA were compared using the Illumina HiSeq 2500 platform.

To map the sequencing reads to the human genome (hg19), we used both vendor-recommended alignment algorithms and ‘universal,’ platform-agnostic aligners. For gene expression quantification, the following aligners were evaluated: STAR<sup>31</sup> (agnostic), ELAND (HiSeq), TMAP (PGM and Proton), GSRM (454) and GMAP (PacBio). With the exception of ELAND, each platform-specific algorithm produced better mapping rates, gene-body coverage evenness and Spearman correlations with PrimePCR quantification (Supplementary Tables 2–4) when compared to STAR applied uniformly across all platforms. However, the universal STAR alignments were used as input for shared junction detection (Supplementary Table 5), since these alignments always showed the lowest mapping error rate (Fig. 1). After mapping, additional processing for quantifying gene counts was performed using the open source r-make package (<http://physiology.med.cornell.edu/faculty/mason/lab/data/r-make>, and Online Methods) to calculate the reads and coverage for each gene feature based on GENCODE (v12) annotation. Quality control data were generated using the fastQC package ([www.bioinformatics.babraham.ac.uk/projects/fastqc](http://www.bioinformatics.babraham.ac.uk/projects/fastqc)) to calculate a large set of performance metrics for sequence quality, gene coverage and transcriptome quantitation and characterization for all platforms (Fig. 1 and Supplementary Figs. 1–23).

### Base qualities, data quality and duplicate rates

Quality Values (QV, a per base accuracy estimate) were calculated for all sample runs, for pre-alignment measures (Supplemental Figs. 1–6) and post-alignment measures (Fig. 1b). Results ranged from Q10 (90% accuracy) to Q60 (99.9999% accuracy) across platforms (Supplementary Figs. 1–6) and revealed three notable trends. First, most platforms show a biased QV distribution in the first 1–16 bases, a known effect from the reverse transcriptase (RT) priming step<sup>32</sup>. This RT bias can also affect the observed GC content (Supplementary Figs. 7–11) and base-frequency data<sup>11,33, 34</sup> (Supplementary Figs. 12–17). Second, similar QV profiles were observed for samples A and B, and across different RNA size fractions. Third, although changes in library preparation techniques and sequencing chemistry for various platforms can affect the QVs, the largest increase in QVs came from the circular consensus sequencing (CCS) for the PacBio data (Supplementary Fig. 2), where median QVs near 40 were observed, though with a wide range of variation. Thus, for most

platforms, the ends of the reads are where most “noise” was observed, but lower QVs also occurred at the beginnings of the reads. This results in a source of bias and noise for RNA-seq data that appears in all platforms and is usually addressed by appropriate sequence trimming.

The QVs for each base of a read, as well as the read length, alignment method and reference sequence quality, can all affect mapping accuracy. To estimate the platform-specific and aligner-specific impact of the sequencing error rate on alignment, we calculated the number of mismatches relative to the hg19 human reference genome, normalized by total mapped bases, for two aligners for each platform (Fig. 1b). These data showed that a tradeoff between higher mapping rate and accuracy can occur for RNA-seq, such as the increased mapping rate with TMAP/GSRM vs. STAR (Supplemental Table 2) that led to a higher empirically derived error rate (Fig. 1b). The most common type of mismatch for HiSeq was single-base substitutions, but the range between all platforms spanned 0.6–7.1%. Insertion/deletion (indel) type mismatch rates were also highly variable between platforms, spanning 0.017–4.4% of all mismatches observed. Moreover, for all platforms, the reported QVs were higher than the empirically derived QVs based on sequence mismatches, similar to the QV-inflation observed for DNA sequencing in the 1000 Genomes Project and GATK<sup>35, 36</sup>.

Previous work in RNA-seq has noted that duplicate reads may be a confounding factor in data analysis because reads with exactly the same start and end may arise from clonal copies produced during library amplification rather than from independently transcribed RNAs in the biological sample<sup>8, 33</sup>. However, unlike DNA sequencing of large diploid genomes, RNA-seq is expected to produce some reads from highly expressed transcripts that begin at the same nucleotide and are thus designated “duplicate.” An assessment of this question over a range of read lengths has not been previously reported, but is facilitated in this study by RNA-seq of the same samples over a range of varying read lengths (Supplementary Figs. 19–23). The read length distributions revealed distinct types for variable-read platforms, including Gaussian (454) and “ski-jump” (Proton and PGM), and the expected uniform lengths for Illumina platforms. Yet, all platforms showed no more than 51% of reads as putative duplicates (Supplementary Fig. 24), with the 454 and PacBio platforms showing the fewest duplicates (12–20%). PacBio library construction does not include any amplification step of the final cDNA library, while the reduced duplication with 454 is likely because the amplification step takes place after template attachment to single beads, so individual molecules in the library have less chance to spawn multiple reads. For the other platforms, this analysis cannot distinguish whether observed duplicates are due to independent transcripts or are a consequence of library amplification, but future datasets based on these same samples will support investigation of this question.

### Coverage of genes

Next we examined the normalized coverage of all GENCODE gene transcripts from 5' to 3' termini for any bias in the number of mapped bases originating from different regions of the transcripts. Almost all samples showed a fairly similar distribution of coverage for genes (Fig. 2). Notably, the ribo-depleted RNA samples, whether degraded or not, consistently showed more-uniform gene coverage than did polyA-selected libraries. The data also

showed “banding” or altered coverage distributions, likely caused by the use of a different library kit version at one of the test sites (C). This indicates that gene coverage can be affected by platform and preparation-dependent factors, but aligners can also play a role (Supplementary Table 3). Finally, the highest and most-uniform coverage of full-length transcripts came from preparing samples with enrichment for both the 3′ polyA tail and an antibody (Ab) for the 5′ methylguanylate cap (5′G cap), combined with long-read technology (see Online Methods for Pacific Biosciences).

### Transcriptome profiling and splice junction detection

We investigated the ability of each platform to reproducibly detect and quantify genes and splice junctions across the transcriptome (Fig. 3). Data were restricted to genes that were observed at all test sites and in all technical replicates for each platform. The platforms showed a median range of 11–39% inter-site CV (Coefficient of Variation) in their quantification of detected genes using normalized gene expression values (Fig. 3a, Supplementary Methods), with HiSeq showing the lowest median CV. The Spearman correlations of normalized transcript levels were measured for samples A and B on different platforms (454, HiSeq, Proton and PGM) across multiple sites for Figure 3b; PacBio was not included because it displayed an (expected) low read count for many genes. The inter-platform correlation was high ( $R^2$  average of 0.83) for the same samples profiled on different platforms, and the intra-platform correlation was even higher ( $R^2$  average greater than 0.86). Each platform was also compared to normalized expression data from an orthogonal quantitation method (PrimePCR, Supplementary Fig. 25), and the Spearman correlations of the log<sub>2</sub> fold differences were ranked as 454 < PGM < Proton, HiSeq, ranging from 0.83 to 0.89.

Next we examined the impact of read depth and length on transcript identification. A clear log-linear relationship was observed between sequence base depth and gene detection (Fig. 3d), showing that increasing the depth of sequencing for any platform is a quick means to find more genes. Characterizations of splice junction detection efficiency and inter-platform agreement have not been previously reported, so to account for each platform’s different read lengths, the effect of total sequenced base depth (rather than read count) was examined for previously annotated and new, unannotated splicing. Splice junction profiling showed an early plateau for detection of known junctions (Fig. 3e). The Proton, PGM and 454 platforms detected more known junctions despite fewer bases sequenced compared to Illumina HiSeq. However, a follow-up experiment with long-read Illumina MiSeq data (2×250 bp paired-end reads) showed a similar boost in junction identification (Supplementary Fig. 26), suggesting that splice junction detection is most affected by read length, rather than library preparation or sequencing chemistry. The ratio of the number of junctions detected as a function of total bases sequenced (junctions/Mb) revealed a wide range of values (Fig. 3f) but clearly demonstrated that longer reads are a more efficient way to capture junctions. This is reflected in the data from the long-read platforms and also in the comparison of the number of junctions detected in the Illumina HiSeq vs. MiSeq data from two aliquots of the same library (22.6 junctions/Mb for HiSeq vs. 33.9 junctions/Mb for MiSeq, Supplemental Fig. 26).

We also characterized the inter-platform agreement of known and novel junctions. The known GENCODE junctions (v12) showed higher inter-platform agreement, with most of these junctions detected by three or more platforms (Fig. 3g, left panel). However, unannotated junctions have lower concordance than known junctions across platforms (Fig. 3g). An examination of these rare isoforms revealed that the lower detection agreement is likely due to their lower expression levels (Supplementary Fig. 27), but they also may represent platform-specific artifacts. Therefore, only unannotated splice junctions observed on at least three platforms (which still includes >20,000 junctions per sample) are reported in this analysis.

These cross-platform splicing data showed that the types of reads dramatically influenced each platform's measure of low abundance transcripts. This effect was apparent for RNA splice isoforms such as SRP9 (Fig. 4a), suggesting that rare-isoform quantification benefits the most from greater read depths (such as from the Illumina HiSeq and Life Technologies Proton). However, uniformity of coverage across exons is improved with long-read technology such as PacBio (Fig. 4a and Supplementary Table 3), despite less read depth. An examination of the size-selected PacBio CCS libraries demonstrated that the polyA+5'G cap enrichment method captured the full lengths of expressed transcripts (Supplementary Fig. 28), with the majority (90%) showing complete transcript sequences in the 1–2 kb range or even longer. These results indicate that a combination of appropriate sample preparation and long reads can readily create cDNA profiles that approach the full-length sequences of mRNAs from complex samples, underlining the utility of long read platforms, despite the lower read depths they may produce<sup>37</sup>.

To examine the ability of each platform to detect differentially expressed genes (DEGs) (Fig. 4b, Supplementary Figs. 29–31), we used limma-voom<sup>38</sup> to perform DEG analysis on the normalized counts for each platform. Although a majority of DEGs were observed by two or more methods, each produced unique DEGs at all statistical significance and fold-change cutoffs (Supplementary Figs. 30, 31). Thus, although high read-depth platforms showed greater DEG overlap, each platform produced unique subsets (from unique systematic effects) of statistically significant DEGs (FDR < 0.05, fold change > 2, Online Methods), ranging from 6–11% of all called DEGs detected uniquely by a platform or preparation method (Fig. 4b, peripheral sets). These instruments span different chemistries, measurement techniques (optical vs. electrical) and base-calling methods, all of which likely play roles in the system-specific noise profiles, as noted in Figures 1–3 and Supplementary Figures 1–24.

### **Influence of library preparation on transcriptome profiles**

To examine other factors that affect DEG measurements, we prepared libraries using both polyA enrichment or ribosomal RNA depletion of the standard samples, and then performed sequencing on the same Illumina HiSeq 2500 instrument. Identical aliquots of the standards (A, B, C and D) were separated into quadruplicate sets for library preparation. All replicate libraries were then sequenced in a multiplexed assay on a full Illumina flow cell. The ribo-depletion library method produced a read source distribution very different from the polyA preparation method (Fig. 5a). The ribo-depleted libraries showed 40–47% of the bases

mapping to introns vs. 7–12% for polyA RNA from the same sample (lower intronic reads were similarly observed for polyA RNA on the other platforms, Supplementary Fig. 32). Both methods produced fairly consistent measures of RNA abundance (FPKM, Online Methods), with a median FPKM difference of only 0.055 between all genes. However, more genes with lower levels of expression were observed with the ribo-depletion method, whereas the polyA libraries contained more highly expressed genes and 3' untranslated regions (3' UTR) Supplementary Fig. 33). As expected, the ribo-depleted libraries were enriched for non-coding RNAs, such as lncRNAs and snoRNAs (Supplementary Table 6), whereas the polyA libraries were enriched for protein-coding genes and mitochondrial genes (Supplementary Tables 6–8)<sup>39</sup>. Sequence annotations in GENCODE currently labeled as “intron” and other categories are likely to change as new non-coding RNAs (or new transcript classes) are identified.

Yet, few overall differences were observed between the polyA and ribo-depleted library preparations in gene quantification and detection of differentially expressed genes. Both data sets were evaluated using alignments from STAR and DEG calculations from limma-voom<sup>38</sup>, and surrogate variable analysis (SVA) was applied for the detection of latent variables (Online Methods)<sup>39</sup>. A pairwise comparison of the average normalized gene expression across replicates of the two library types for the four standard samples showed high Spearman correlation coefficients (sample A: 0.91, B: 0.93, C: 0.92, D: 0.93). The overall numbers of DEGs detected between the biologically distinct samples (A vs. B, A vs. D, etc.) were also consistent between library preparation methods (Fig. 5b, 5c). These DEG data were then compared to results from 802 TaqMan assays for these same RNA samples (GEO dataset GSE5350)<sup>10</sup>. Both library types had similar accuracy as measured by Matthews correlation coefficient (MCC, Fig. 5d)<sup>40, 41</sup>, which is a joint measure of the assay's sensitivity and specificity. The corresponding DEGs without SVA analysis show similar but slightly lower overlap percentage and MCC (Supplementary Fig. 33). The median MCC is 0.659 before SVA and 0.678 after SVA, with an average increase of 0.015. Also, the percentage of shared DEGs ranges from 67–81% at FDR < 0.01 and fold-change > 2, and similarly ranges from 68–81% after SVA. However, the synthetic RNAs spiked into these samples (ERCC controls) performed slightly better in the ribo-depletion protocol than the polyA-enrichment protocol (mean  $R^2 = 0.91$  and  $0.82$ , respectively), although these ranges of correlation to TaqMan were similar to that observed for ERCCs sequenced on the PGM, where the mean  $R^2 = 0.78$  (Supplementary Figs. 34, 35).

### Impact of RNA degradation on transcriptome profiling

As polyA and ribo-depleted gene quantifications were similar, we sought to test the effect of ribo-depletion on “low quality” or degraded RNAs. The reference samples A and B were degraded using heat, sonication or RNase-A until all samples showed a high level of degradation when evaluated on the Agilent Bioanalyzer 2100 (RIN 2.0, Online Methods). Samples were ribo-depleted before library preparation and sequenced on the HiSeq platform at multiple sites. Multiple metrics indicated that the degraded RNA performed as well as the polyA-enriched or ribo-depleted libraries from intact RNA. First, sequencing of the degraded RNA, after ribo-depletion, fully covered the gene bodies (Fig. 2) and, similar to ribo-depleted libraries from intact RNA, more reads mapped to intronic areas of the genome



(Supplementary Fig. 32). Second, the degraded RNA showed minor differences in gene detection or DEG accuracy, with high Spearman correlation ( $R^2 > 0.96$ , Fig. 3c) in expression comparisons to intact RNA samples. In addition, a comparison to the orthogonal PrimePCR dataset showed that the degraded RNA analysis was highly correlated (Pearson  $R^2 > 0.83$ ) to the corresponding intact samples (Supplementary Table 4). However, the degraded RNA did have a lower Spearman rank-order correlation with quantitative PCR for the expression differences detected between samples A and B. The Spearman correlation was highest for heat degradation ( $R^2 = 0.83$ , AH), followed by RNase A ( $R^2 = 0.79$ , AR), and then sonication ( $R^2 = 0.74$ , AS) (Supplementary Figs. 36a–c). Comparison of the results from one degraded sample to the results from one intact sample, repeated at multiple laboratories (sites L, V and R), also produced an overall high average Spearman correlation coefficient (0.80, Supplementary Fig. 36d). These data indicate that although appropriate library preparation of degraded RNA can produce accurate expression measurements (Supplementary Fig. 36), but mixing intact and degraded samples (or samples degraded during different types of tissue processing) should be avoided.

## Discussion

This ABRF-NGS Study represents, to our knowledge, the largest reported cross-platform, cross-protocol, and cross-site examination of RNA-seq data performed to date. The results provide a unique opportunity to examine various aspects of the transcriptome, including the intra- and inter-site coefficients of variance of gene detection, gene expression quantification and RNA splicing between sequencing platforms, as well as the ability of long read lengths to enable complete isoform characterization. Comparisons of platform-specific aligners with STAR showed that mapping rates, error rates and transcript coverage are larger concerns when considering inter-platform data than is gene quantification. As such, the use of different alignment algorithms will have different influences on comparisons between experiments depending on the metric studied, and the importance of ‘bioinformatics noise’ can be placed alongside technical and biological noise as key factors in experimental design. Finally, the results expanded previous work<sup>26</sup> by showing that gene detection and quantification with highly fragmented or degraded RNA samples (from three types of degradation) is strikingly similar to intact RNA, once ribosomal RNA is removed.

This study found similar RNA-seq results between the various NGS platforms and similar ranges in coefficients of variance across lab sites for each platform. These results indicate that both long- and short-read technologies measure gene expression with similar levels of statistical variation, although they show a ten-fold variation for error rates in indels. Using normalized gene expression as a comparison measure, we found high intra-platform consistency ( $R^2 > 0.86$ ) and high inter-platform concordance ( $R^2 > 0.83$ ) measured by Spearman rank correlation (Fig. 3b). However, the results clearly show that deeper sequencing of the transcriptome is needed to reveal low abundance transcripts and splice junctions, indicating that read depth should be a key consideration when experimental goals include rarely expressed genes, coverage of introns and non-polyadenylated targets. Very deep sampling is not currently cost-effective with long-read platforms such as PacBio or 454 (Table 1), and thus the best discovery platforms for low-abundance targets are currently the

shorter read platforms, as they can cover wider dynamic range of RNA molecules (i.e., generate more reads per sample).

Despite lower read depths and higher costs, the longer read NGS technologies have the best ability to efficiently catch the vast majority of known splice junctions (Fig. 3d–g), indicating that they can be an effective means to annotate splicing complexity. The ABRF-NGS Study's results include a wealth of putative novel splice junctions, with more than one million such junctions observed in at least one platform (Gene Expression Omnibus GSE46876). These putative novel splice junctions displayed greater inter-platform disparity than the known splice junctions (Fig. 3e). This difference was likely due to the challenge of correctly predicting novel isoforms and also to the possibly high false-positive rate of such predictions, which is expected given their lower expression levels. However, a substantial number of the previously unannotated, predicted junctions are likely genuine, as they were observed using multiple platforms. The resulting data sets nearly double the catalog of splice junctions for these RNA standard samples. The junctions discovered on multiple platforms can be used alone or with previous data for future algorithm design and assay optimization, and as positive controls, to advance splicing isoform characterization by RNA-seq<sup>14, 42-44</sup>.

Perhaps most notably, the data demonstrated that results from polyA-enriched and ribo-depleted RNA libraries, and even libraries made from severely degraded RNAs, are comparable. Given sufficient depth of sequencing, results from ribo-depleted libraries can include almost all of the differentially detected genes identified by the polyA preparation method, without loss of sensitivity or specificity. This was evident not only in the overlap of DEGs, but also in comparisons to TaqMan and PrimePCR data. Furthermore, a near-complete reconstruction of the transcriptome profile was observed when using degraded RNA in the ribo-depletion protocol, with some variation between degradation treatments, as judged by correlations to the expression abundances measured in intact samples A and B by quantitative PCR and by the uniform coverage of full transcript lengths. Similar degraded RNA results were recently reported<sup>26</sup>, suggesting that low quality samples can now be considered for reliable RNA-seq expression profiling. This should support studies using old, degraded or fragmented RNAs, such as those from formalin-fixed, paraffin-embedded (FFPE) tissues in clinical archives. Although the degraded RNA samples were run only on the HiSeq platform, the clear utility of such an approach should spur the development of similar degraded RNA resources for analyses on all sequencing platforms.

However, despite their overall similarities, distinct transcriptomes are represented in libraries prepared by polyA enrichment, ribo-depletion or combined polyA and 5'G cap enrichment. The dual enrichment method for PacBio libraries provided superior 5' to 3' coverage of the sequenced transcripts, as illustrated by comparisons across platforms for genes consistently detected by PacBio (Supplementary Fig. 37). The revised version of the Illumina library kit (v2 vs. v3) includes built-in ribo-depletion and tags cDNA strand orientation, and the two protocols produced differences in gene-body coverage. A comparison of polyA and ribo-depleted libraries showed different detection of nonpolyadenylated transcripts, 3'UTRs and introns. The former is an intentional consequence of the enrichment protocol, but it is not clear if the 3'UTR coverage bias is due to different efficiencies of priming during reverse transcription or to skewed sampling

caused by a higher concentration of structural and non-coding RNAs in ribo-depleted libraries. Owing to the higher rate of intron-mapped reads, RNA-seq of total RNA will require greater read depths for ribo-depleted libraries (~2.5X) than for polyA libraries to achieve equal coverage of exons. Transcriptome measurement variations demonstrated between the reference datasets are easily avoided by consistently using the same protocols, platform, and analysis pipeline for all samples in an experiment. Nonetheless, if this is not possible, surrogate variable analysis enabled removal of latent variables from the data for ribo-depleted and polyA-enriched libraries, producing nearly indistinguishable lists of DEGs and illustrating the utility of surrogate variable analysis as a powerful and strongly recommended method for ameliorating the effects of inter-batch and cross-protocol noise.

The results presented here also highlight additional variables that should be considered when aligning library protocols and platforms with research goals. The reported QV values of all platforms are all higher than empirically derived error rates, indicating that a splicing-aware, base quality score recalibration may be needed for RNA-seq, as is already done for DNA-seq with GATK. Long-read sequencing effectively cataloged splicing isoforms, but had less dynamic range for transcript quantitation and discovery due to lower read depths. The use of the ERCCs is generally recommended as a good QC metric check, but these standards performed better in ribo-depleted libraries than in polyA libraries, and this should also be considered during experimental design. In summary, the priorities for biological interpretation are essential when considering the protocols and methods that will be used in an RNA-seq experiment. Some of these priorities are summarized in Table 1, which provides a cross platform summary of the strengths and relative costs of the sequencing technologies included in this study.

The ABRF-NGS Study is not intended to be a “bake-off” between NGS platforms, but rather is an effort to establish a useful reference data set for each platform which will assist laboratories in improving their methods and in evaluating new chemistries, protocols and instruments. It is encouraging that comparison of gene expression quantification, including results from intra-platform, inter-platform, inter-protocol and even inter-aligner comparisons, demonstrated high correlations overall. This result suggests broader inter-study analyses and data mining can be successfully carried out across multiple platforms despite intrinsic differences between technologies, methods and aligners.

Reference data resources, such as the results from this ABRF-NGS Study, are key to understanding the effects of variable sample quality, changes to platform protocols and the adoption of new technologies. Given the rapid pace of advancement in sequencing technologies, techniques and bioinformatics tools, the methods and data described here can facilitate the development of best practices for gene quantification, isoform characterization, dynamic range comparisons, managing inter-site and intra-site variation, analysis pipeline refinement, and cross-platform testing of transcriptome hypotheses. These data can also be used to address other aspects of RNA-seq, including polymorphism detection, allele-specific expression, intron retention, RNA editing and gene fusions, and provide an immediately useful resource that can complement current databases, such as the RNA-Seq Atlas<sup>45</sup>. These and other applications, especially clinical molecular diagnostics that rely on nucleic acid biomarkers, will require a level of technical stability across time and both within and

between studies, which this study helps to establish. Reference data resources are key to monitoring platform stability, and widespread adoption of standard samples and routine reference benchmarking are challenges that must be addressed to advance genomics technologies further.

## Supplementary Material

Refer to Web version on PubMed Central for supplementary material.

## Acknowledgments

We greatly appreciate the contribution and distribution of reference sample RNA from Leming Shi (FDA) and his valuable interactions to assist in the planning of this study. This work was supported with funding from the National Institutes of Health (NIH), including R01HG006798, R01NS076465, R24RR032341, as well as funds from the Irma T. Hirschl and Monique Weill-Caulier Charitable Trusts and the STARR Consortium (I7-A765).

We thank the following contributors for their technical wisdom, including laboratory expertise, data analysis and bioinformatics contributions, and technical design guidance and consultation. Without their help, this study would not have been possible: Diane Stopka (Memorial Sloan-Kettering Cancer Institute), Gregory Grove (Penn State Univ.), Daniel Hannon (Penn State Univ.), Kristine Jones (NIH/NCI/SAIC), Castle Raley (NIH/NCI/SAIC), Henriette O'Geen (UC Davis), Danman Zheng (Univ. Illinois-Urbana), Oanh Nguyen (UC Davis), Zhi-Wei Lu (UC Davis), Jezra Spisak (Cornell Univ.), Dawei Lin (NIH/NIAID), Jaroslaw Pillardy (Cornell Univ.), Po-Yen Wu (Georgia Institute of Technology), John Phan (Emory Univ.), Dayna Oschwald (New York Genome Center), Hugh Arnold (Perkin Elmer), Selene Tyndale (Univ. Southern California), Helen Truong (Univ. Southern California), Yanping Zhang (Univ. Florida), Nedka Panayotova (Univ. Florida), David Moraga (Univ. Florida), Savita Shanker (Univ. Florida), and Natalie Barker (U.S. Army Environmental Quality Research Program).

We would also like to thank the platform vendors, Illumina, Life Technologies, Pacific Biosciences and Roche Life Sciences, for their support of this study, and their distinguished scientists for providing technical expertise and assistance in study designs, protocols, new methods development and significant contributions of reagents and sequencing kits. In particular, alphabetically by vendor: Gary Schroth (Illumina); Michael Gallad, Jeff Smith, Tom Bittick and Robert Setterquist (Life Technologies); Jonas Korlach, Steve Turner and Elizabeth Tseng (Pacific Biosciences); and Karin Fredrickson and Clotilde Teiling (Roche Life Sciences).

We are sincerely appreciative of the Association of Biomolecular Resource Facilities (ABRF) for supporting this study and the contributing ABRF Research Groups. Special thanks to our ABRF Executive Board liaison, Anoja Perera (Stowers Institute for Medical Research), and to Michelle Carr (Cornell Univ.) for administrative support.

## References

1. Wang ET, et al. Alternative isoform regulation in human tissue transcriptomes. *Nature*. 2008; 456:470–476. [PubMed: 18978772]
2. Nagalakshmi U, Waern K, Snyder M. RNA-Seq: a method for comprehensive transcriptome analysis. *Curr Protoc Mol Biol*. 2010; 11:11–13. Chapter 4, Unit 4. [PubMed: 20069539]
3. Liu S, Lin L, Jiang P, Wang D, Xing Y. A comparison of RNA-Seq and high-density exon array for detecting differential gene expression between closely related species. *Nucleic Acids Res*. 2011; 39:578–588. [PubMed: 20864445]
4. Marioni JC, Mason CE, Mane SM, Stephens M, Gilad Y. RNA-seq: an assessment of technical reproducibility and comparison with gene expression arrays. *Genome Res*. 2008; 18:1509–1517. [PubMed: 18550803]
5. Mortazavi A, Williams BA, McCue K, Schaeffer L, Wold B. Mapping and quantifying mammalian transcriptomes by RNA-Seq. *Nat. Methods*. 2008; 5:621–628. [PubMed: 18516045]
6. Liu L, et al. Comparison of next-generation sequencing systems. *J. Biomed. Biotechnol*. 2012; 2012:251364. [PubMed: 22829749]
7. Ratan A, et al. Comparison of sequencing platforms for single nucleotide variant calls in a human sample. *PLoS one*. 2013; 8:e55089. [PubMed: 23405114]

8. Quail MA, et al. A tale of three next generation sequencing platforms: comparison of Ion Torrent, Pacific Biosciences and Illumina MiSeq sequencers. *BMC Genomics*. 2012; 13:341. [PubMed: 22827831]
9. Loman NJ, et al. Performance comparison of benchtop high-throughput sequencing platforms. *Nat. Biotechnol.* 2012; 30:434–439. [PubMed: 22522955]
10. Shi L, et al. The MicroArray Quality Control (MAQC) project shows inter- and intraplatform reproducibility of gene expression measurements. *Nat. Biotechnol.* 2006; 24:1151–1161. [PubMed: 16964229]
11. (MAQC-3), S.Q.C.C. Power and limitations of RNA-Seq. *Nature biotechnology*. 2014
12. t Hoen PA, et al. Reproducibility of high-throughput mRNA and small RNA sequencing across laboratories. *Nature biotechnology*. 2013
13. Tarazona S, Garcia-Alcalde F, Dopazo J, Ferrer A, Conesa A. Differential expression in RNAseq: a matter of depth. *Genome research*. 2011; 21:2213–2223. [PubMed: 21903743]
14. Katz Y, Wang ET, Airoidi EM, Burge CB. Analysis and design of RNA sequencing experiments for identifying isoform regulation. *Nat. Methods*. 2010; 7:1009–1015. [PubMed: 21057496]
15. Labaj PP, et al. Characterization and improvement of RNA-Seq precision in quantitative transcript expression profiling. *Bioinformatics*. 2011; 27:i383–391. [PubMed: 21685096]
16. McIntyre LM, et al. RNA-seq: technical variability and sampling. *BMC Genomics*. 2011; 12:293. [PubMed: 21645359]
17. Huang R, et al. An RNA-Seq strategy to detect the complete coding and non-coding transcriptome including full-length imprinted macro ncRNAs. *PloS one*. 2011; 6:e27288. [PubMed: 22102886]
18. Wang Z, Gerstein M, Snyder M. RNA-Seq: a revolutionary tool for transcriptomics. *Nat Rev Genet*. 2009; 10:57–63. [PubMed: 19015660]
19. Toung JM, Morley M, Li M, Cheung VG. RNA-sequence analysis of human B-cells. *Genome Res*. 2011; 21:991–998. [PubMed: 21536721]
20. Roberts A, Pimentel H, Trapnell C, Pachter L. Identification of novel transcripts in annotated genomes using RNA-Seq. *Bioinformatics*. 2011; 27:2325–2329. [PubMed: 21697122]
21. Angeletti RH, et al. Research technologies: fulfilling the promise. *Faseb J*. 1999; 13:595–601. [PubMed: 10094920]
22. Moelans CB, Oostenrijk D, Moons MJ, van Diest PJ. Formaldehyde substitute fixatives: effects on nucleic acid preservation. *J Clin Pathol*. 2011; 64:960–967. [PubMed: 21715573]
23. Opitz L, et al. Impact of RNA degradation on gene expression profiling. *BMC Med Genomics*. 2010; 3:36. [PubMed: 20696062]
24. Morlan JD, Qu K, Sinicropi DV. Selective depletion of rRNA enables whole transcriptome profiling of archival fixed tissue. *PloS one*. 2012; 7:e42882. [PubMed: 22900061]
25. Pareek CS, Smoczynski R, Tretyn A. Sequencing technologies and genome sequencing. *J Appl Genet*. 2011; 52:413–435. [PubMed: 21698376]
26. Adiconis X, et al. Comparative analysis of RNA sequencing methods for degraded or low-input samples. *Nat Methods*. 2013; 10:623–629. [PubMed: 23685885]
27. Boland JF, et al. The new sequencer on the block: comparison of Life Technology's Proton sequencer to an Illumina HiSeq for whole-exome sequencing. *Human genetics*. 2013
28. Glenn TC. Field guide to next-generation DNA sequencers. *Mol. Ecol. Resour*. 2011; 11:759–769. [PubMed: 21592312]
29. Jiang L, et al. Synthetic spike-in standards for RNA-seq experiments. *Genome research*. 2011; 21:1543–1551. [PubMed: 21816910]
30. Zook JM, Samarov D, McDaniel J, Sen SK, Salit M. Synthetic spike-in standards improve run-specific systematic error analysis for DNA and RNA sequencing. *PloS one*. 2012; 7:e41356. [PubMed: 22859977]
31. Dobin A, et al. STAR: ultrafast universal RNA-seq aligner. *Bioinformatics*. 2013; 29:15–21. [PubMed: 23104886]
32. Hansen KD, Brenner SE, Dudoit S. Biases in Illumina transcriptome sequencing caused by random hexamer priming. *Nucleic Acids Res*. 2010; 38:e131. [PubMed: 20395217]

33. Aird D, et al. Analyzing and minimizing PCR amplification bias in Illumina sequencing libraries. *Genome Biol.* 2011; 12:R18. [PubMed: 21338519]
34. Risso D, Schwartz K, Sherlock G, Dudoit S. GC-content normalization for RNA-Seq data. *BMC bioinformatics.* 2011; 12:480. [PubMed: 22177264]
35. Genomes Project C, et al. An integrated map of genetic variation from 1,092 human genomes. *Nature.* 2012; 491:56–65. [PubMed: 23128226]
36. McKenna A, et al. The Genome Analysis Toolkit: a MapReduce framework for analyzing nextgeneration DNA sequencing data. *Genome research.* 2010; 20:1297–1303. [PubMed: 20644199]
37. Sharon D, Tilgner H, Grubert F, Snyder M. A single-molecule long-read survey of the human transcriptome. *Nat Biotechnol.* Nov; 2013 31(11):1009–14. [PubMed: 24108091]
38. Smyth, GK. *Bioinformatics and Computational Biology Solutions Using R and Bioconductor.* Gentleman, R.; Carey, V.; Huber, W.; Irizarry, R.; Dudoit, S., editors. Springer; New York: 2005. p. 397-420.
39. Cui P, et al. A comparison between ribo-minus RNA-sequencing and polyA-selected RNaseq. *Genomics.* 2010; 96:259–265. [PubMed: 20688152]
40. Leek JT, Johnson WE, Parker HS, Jaffe AE, Storey JD. The sva package for removing batch effects and other unwanted variation in high-throughput experiments. *Bioinformatics.* 2012; 28:882–883. [PubMed: 22257669]
41. Baldi P, Brunak S, Chauvin Y, Andersen CA, Nielsen H. Assessing the accuracy of prediction algorithms for classification: an overview. *Bioinformatics.* 2000; 16:412–424. [PubMed: 10871264]
42. Shi L, et al. The MicroArray Quality Control (MAQC)-II study of common practices for the development and validation of microarray-based predictive models. *Nature biotechnology.* 2010; 28:827–838.
43. Haas BJ, Zody MC. Advancing RNA-Seq analysis. *Nature biotechnology.* 2010; 28:421–423.
44. Wenger Y, Galliot B. RNAseq versus genome-predicted transcriptomes: a large population of novel transcripts identified in an Illumina-454 Hydra transcriptome. *BMC Genomics.* 2013; 14:204. [PubMed: 23530871]
45. Pipes L, et al. The non-human primate reference transcriptome resource (NHPRT) for comparative functional genomics. *Nucleic acids research.* 2013; 41:D906–914. [PubMed: 23203872]
46. Krupp M, et al. RNA-Seq Atlas--a reference database for gene expression profiling in normal tissue by next-generation sequencing. *Bioinformatics.* 2012; 28:1184–1185. [PubMed: 22345621]
47. Van Peer G, Mestdagh P, Vandesompele J. Accurate RT-qPCR gene expression analysis on cell culture lysates. *Sci. Rep.* 2012; 2:222. [PubMed: 22355736]
48. Hellemans J, Mortier G, De Paepe A, Speleman F, Vandesompele J. qBase relative quantification framework and software for management and automated analysis of real-time quantitative PCR data. *Genome Biol.* 2007; 8:R19. [PubMed: 17291332]
49. Bustin SA, et al. The MIQE guidelines: minimum information for publication of quantitative realtime PCR experiments. *Clin. Chem.* 2009; 55:611–622. [PubMed: 19246619]
50. Robinson MD, McCarthy DJ, Smyth GK. edgeR: a Bioconductor package for differential expression analysis of digital gene expression data. *Bioinformatics.* 2010; 26:139–140. [PubMed: 19910308]
51. Robinson MD, Smyth GK. Moderated statistical tests for assessing differences in tag abundance. *Bioinformatics.* 2007; 23:2881–2887. [PubMed: 17881408]
52. Robinson MD, Smyth GK. Small-sample estimation of negative binomial dispersion, with applications to SAGE data. *Biostatistics.* 2008; 9:321–332. [PubMed: 17728317]
53. Leek JT, Storey JD. Capturing heterogeneity in gene expression studies by surrogate variable analysis. *PLoS Genet.* 2007; 3:1724–1735. [PubMed: 17907809]
54. Wang L, Wang S, Li W. RSeQC: quality control of RNA-seq experiments. *Bioinformatics.* 2012; 28:2184–2185. [PubMed: 22743226]

55. Canales RD, et al. Evaluation of DNA microarray results with quantitative gene expression platforms. *Nat. Biotechnol.* 2006; 24:1115–1122. [PubMed: 16964225]
56. Dvinge H, Bertone P. HTqPCR: high-throughput analysis and visualization of quantitative realtime PCR data in R. *Bioinformatics.* 2009; 25:3325–3326. [PubMed: 19808880]

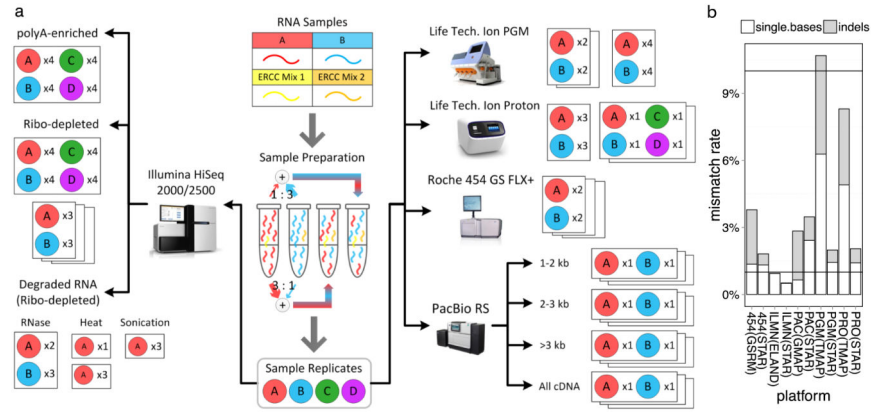


**Figure 1. Experimental design and sequencing platforms**  
 (a) Two standard RNA samples (A = Universal Human Reference RNA and B = Human Brain Reference RNA) were combined with two sets of synthetic RNAs (ERCCs) to prepare a set of samples to be sequenced on five platforms: Illumina (ILMN) HiSeq 2000/2500, Life Technologies Personal Genome Machine (PGM), Life Technologies Proton (PRO), Pacific Biosciences (PacBio) RS (PAC), and the Roche 454 GS FLX+. Additional RNA samples were also generated: samples C and D were prepared as defined mixtures of A and B, while other aliquots of A and B were degraded by three methods. All these additional samples were ribo-depleted for RNA-seq on the HiSeq platform. The number of technical replicates (x2, x3 or x4) of each sample set is indicated for each platform and method. (b) Stacked bar plots of the sequencing platforms' mismatch rates (y-axis) for single-base mismatches (white) and insertions/deletions (indels, grey) based on different aligners for each platform (x-axis). Q10 (90% accuracy) and Q20 (99% accuracy) are shown as the top and bottom line, respectively.



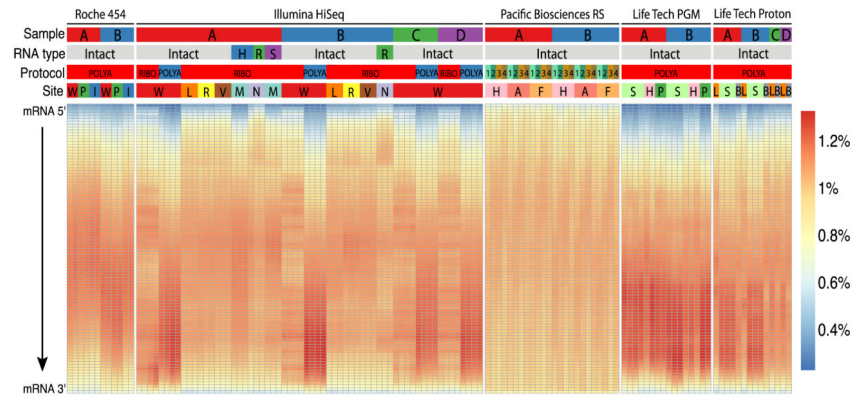


**Figure 2. Transcript coverage across all genes detected**

Each gene was examined as a set of 100 adjacent segments (percentiles of total transcript length). The relative number of reads that map to each segment was then plotted for each sample, platform, and technique (percent of all library reads per segment, see heatmap color key). Samples are categorized by five parameters (top): NGS platforms: Roche 454 GS FLX+, Illumina HiSeq 2000/2500, Pacific Biosciences RS, Life Technologies PGM and Proton; input RNA sample: samples A (red), B (blue), C (green), and D (purple); RNA type: intact or degraded by heat (H, blue), RNase (R, green) or sonication (S, purple); library protocol: polyA enrichment, ribosomal RNA depletion (ribo) or polyA plus 5' cap enrichment with (1, 2, 3) or without (4) size fractionation; and site: 14 core facility sequencing laboratories. Most platforms showed less coverage at the 5' and 3' ends of the transcripts. Details on sequencing platforms, site abbreviations, sample type chemistries, and library preparations are listed in Table 2.

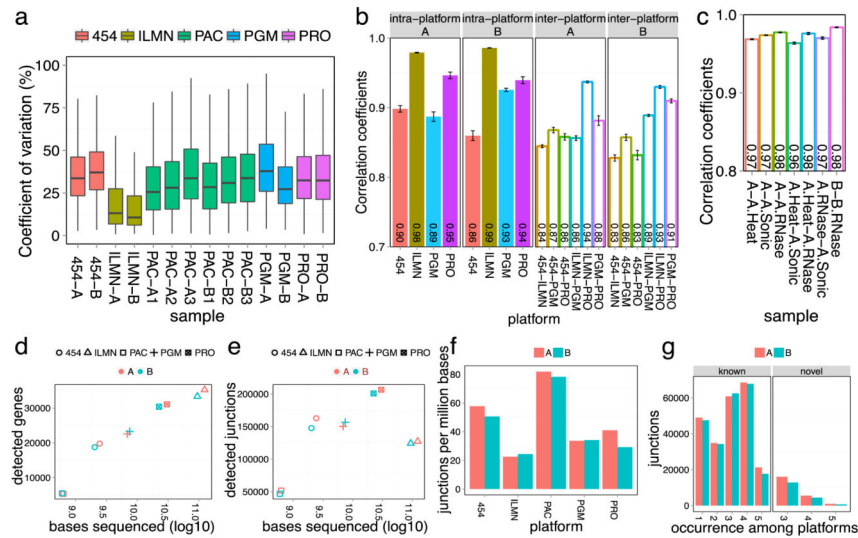


**Figure 3. Intra- and inter-platform variation of RNA-seq transcript metrics**

The coefficients of variation (CV) of various metrics for transcripts detected across all sites were calculated for the Roche 454 GS FLX+, Illumina HiSeq 2000/2500 (ILMN), Pacific Biosciences RS (PAC), and Life Technologies PGM and Proton (PRO). (a) Inter-site CV of normalized gene expression for transcripts detected across all sites. The median CV for number of genes detected ranged from 10.70-38.68%, with many outlier genes present for each platform. (b) Inter-platform and intra-platform normalized gene expression Spearman correlation coefficients for samples A and B. (c) The degraded RNA profiles match the corresponding intact RNA profiles from HiSeq RNA-seq with very high correlation coefficients (0.975). Error bars are standard error of the mean. (d-e) Sequenced bases ( $\log_{10}$ ) were plotted against the number of detected genes or the number of detected splice junctions for known GENCODE junctions. (f) More efficient splice junction detection (y-axis, number of junctions/Mb of sequence) was observed for long read platforms (PAC, 454). Detection efficiencies were calculated at comparable scales by constraining the total number of bases used from each platform to a range of  $630\text{-}5451 \times 10^6$ . (g) Most known junctions were detected by three or more platforms, indicating concordance among RNA-seq methods (left panel). The novel junctions (right) defined by independent observation on three or more platforms were less numerous than known junctions.

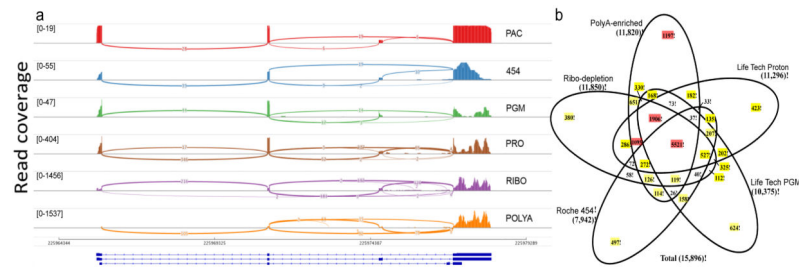


**Figure 4. Inter-platform consistency of splicing and differential expression analysis**

(a) As a representative plot for RNA splicing, transcripts from the SRP9 gene are shown in a sashimi plot across five platforms and two Illumina library protocols. Pacific Biosciences (PAC), Roche 454 (454), and Life Technologies Ion PGM (PGM) detected the two most abundant isoforms. Life Technologies Proton (PRO) and Illumina ribo-depletion (RIBO) or polyA-enriched (POLYA) methods also detected a third isoform. PAC showed more uniform sequencing depth across the gene body. Read coverage as measured by the range of 19-1537 (coverage) is indicated in brackets. (b) Starting from the set of genes detected at any expression level on all platforms, the numbers of A vs. B differentially expressed genes uniquely or repeatedly detected at statistically significant thresholds (FDR <0.05 and fold change >2) are shown; sets of greater than 1000 genes are indicated in red, 100-999 in yellow.

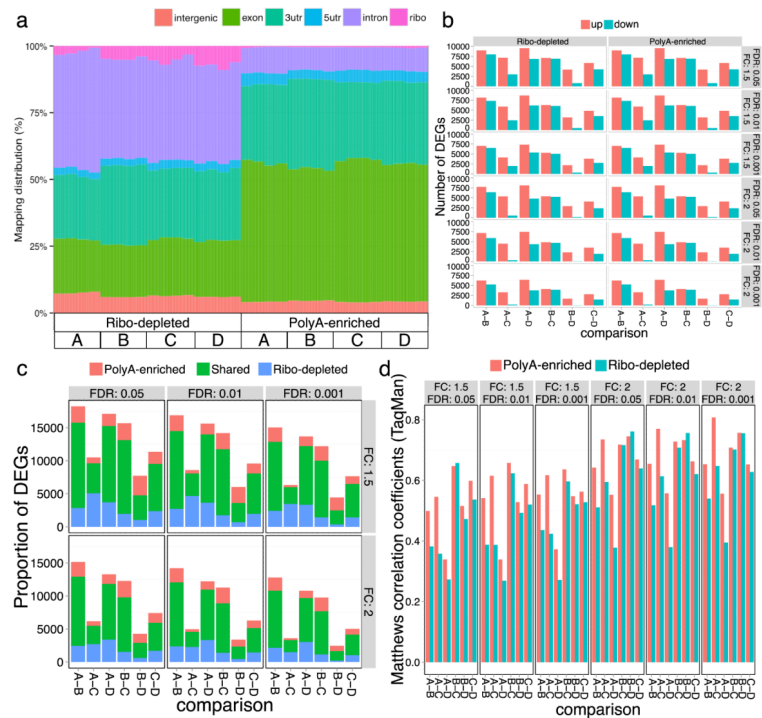


**Figure 5. Differentially expressed genes in ribo-depleted and polyA-enriched libraries**  
 (a) The percentage of reads that map to various gene sequence categories was plotted. A greater number of intronic reads from ribo-depleted libraries was observed. The sequence type and read distribution of gene features detected in polyA-enriched and ribo-depleted libraries from the same sample were examined using GENCODE (v12) annotations. Mitochondrial RNA reads are present at trace levels (<0.1%, data not shown). (b) Differentially expressed genes (DEGs) were detected in all pairwise comparisons of the original (A, B) and mixed samples (C, D); (c) results were similar for both library types from the common set of detected genes at all fold-change (FC) and false discovery rate (FDR) thresholds tested. (d) Both library types show similar accuracy as evidenced by Matthews Correlation Coefficients (MCC) with RT-qPCR assays (see Suppl. Fig. 29b for expanded data). A subset of GENCODE mapped reads was used from each library (mean = 37.6 million reads, S.D. = 2.07 million per replicates) to ensure the same number of exon-mapped reads per sample was compared between all replicates.

Table 1

Summary of RNA-seq platforms as deployed in the ABRF-NGS Study.

Vendor	Instrument	Version	Run Time (hours)	Read Length (mean)	Reads per Run (million)	Yield per Run	Cost per Run (\$) <sup>1</sup>	Cost per Mb (\$)	Paired-end	Application	Strengths
Illumina	HiSeq 2000	High Output	132	50	6,000	300 Gb <sup>2</sup>	18,725.00	0.06	Yes	Gene expression; splice junction detection; variant calling; fusions	Deep read counts for transcript quantification
Illumina	HiSeq 2500	High Output	132	50	6,000	300 Gb <sup>2</sup>	18,725.00	0.06	Yes	as above	as above
Illumina	MiSeq	v2 kit	39	250	30	7.5 Gb	982.75	0.13	Yes	Splice junction detection; variant calling	Rapid transcript quantification and variant detection
Life Technologies	PGM	318 chip	7.3	176	6	1.056 Gb	749.00	0.71	No	Splice junction detection; variant calling	Rapid transcript quantification and variant detection
Life Technologies	Proton	Proton I chip	2 to 4	81	70	5.67 Gb	834.00	0.15	No	Gene expression; variant calling	Good read depth and length for transcript quantification
Pacific Biosciences	RS	RS	0.5 to 2	1,289	0.03	38.67 Mb	136.38	3.53	No	Splice junction detection; full length gene coverage	Extended read lengths
Roche	454	Genome Sequencer FLX+	20	686	1	686 Mb	5,985.00	8.72	No	Splice junction detection	Read length

<sup>1</sup> sequencing reaction reagents, at academic list price U.S. dollars, and does not include library preparation reagents, labor, data storage or analysis, equipment or maintenance;

<sup>2</sup> one sequencing run using 2 flowcells. Pacific Biosciences is calculated based on CCS reads; Gb: billion bases, Mb: million bases

**Table 2**

Sequencing platforms, chemistries and library preparations.

Illumina HiSeq2000/2500 and MiSeq						
Labs	Samples	Libraries per Sample	Preparation	Read Length	Number of Reads per Library	Output (Mb)
1(L)	MAQC A <sup>1</sup>	3	Ribo-depleted	100 bp (2 x 50)	386,726,967	38,673
	MAQC B <sup>1</sup>	3	Ribo-depleted	100 bp (2 x 50)	251,724,566	25,172
2(R)	MAQC A <sup>1</sup>	3	Ribo-depleted	100 bp (2 x 50)	229,131,233	22,913
	MAQC B <sup>1</sup>	3	Ribo-depleted	100 bp (2 x 50)	229,591,730	22,959
	MAQC B <sup>1</sup>	1	Ribo-depleted	500 bp (2 x 250)	7,848,217	3,924
3(V)	MAQC A <sup>1</sup>	3	Ribo-depleted	100 bp (2 x 50)	207,603,620	20,760
	MAQC B <sup>1</sup>	3	Ribo-depleted	100 bp (2 x 50)	239,930,780	23,993
4(N)	MAQC A <sup>1,3</sup>	2	Ribo-depleted	100 bp (2 x 50)	215,903,801	21,590
	MAQC B <sup>1,3</sup>	3	Ribo-depleted	100 bp (2 x 50)	219,257,190	21,926
	MAQC A <sup>1,4</sup>	1	Ribo-depleted	100 bp (2 x 50)	183,811,383	18,381
5(M)	MAQC A <sup>1,4</sup>	3	Ribo-depleted	100 bp (2 x 50)	386,726,967	38,673
	MAQC A <sup>1,5</sup>	3	Ribo-depleted	100 bp (2 x 50)	181,740,643	18,174
6(W)	MAQC A <sup>2</sup>	4	Ribo-depleted	100 bp (2 x 50)	128,133,887	12,813
	MAQC B <sup>2</sup>	4	Ribo-depleted	100 bp (2 x 50)	137,096,343	13,710
	MAQC C <sup>2</sup>	4	Ribo-depleted	100 bp (2 x 50)	142,135,538	14,214
	MAQC D <sup>2</sup>	4	Ribo-depleted	100 bp (2 x 50)	128,040,437	12,804
	MAQC A <sup>2</sup>	4	polyA-enriched	100 bp (2 x 50)	106,762,840	10,676
	MAQC B <sup>2</sup>	4	polyA-enriched	100 bp (2 x 50)	111,430,017	11,143
	MAQC C <sup>2</sup>	4	polyA-enriched	100 bp (2 x 50)	108,582,900	10,858
	MAQC D <sup>2</sup>	4	polyA-enriched	100 bp (2 x 50)	105,978,082	10,598
Life Technologies Ion Torrent PGM and Proton						
Labs	Samples <sup>6</sup>	Libraries per Sample	Preparation <sup>7</sup>	Median Read Length	Mean Number of Reads	Output (Mb)
1(P) Ion PGM	MAQC A	2	polyA-enriched	161	5,323,672	857
	MAQC B	2	polyA-enriched	184	5,802,563	107
	ERCC 1	1	polyA-enriched	189	4,188,385	792
	ERCC 2	1	polyA-enriched	158	3,231,475	511
	ERCC 1	1	polyA-enriched	180	4,442,093	800
	ERCC 2	1	polyA-enriched	189	4,310,663	815

---

**Life Technologies Ion Torrent PGM and Proton**


---

Labs	Samples <sup>6</sup>	Libraries per Sample	Preparation <sup>7</sup>	Median Read Length	Mean Number of Reads	Output (Mb)
2(H) Ion PGM	MAQC A	3	polyA-enriched	128	3,374,068	445
	MAQC B	3	polyA-enriched	129	3,409,662	436
	ERCC 1	2	polyA-enriched	152	2,538,594	810
	ERCC 2	2	polyA-enriched	112	2,119,884	514
	VL A	1	polyA-enriched	187	3,965,022	770
	VL B	1	polyA-enriched	162	4,138,326	687
3(S) Ion PGM	MAQC A	3	polyA-enriched	198	5,049,998	1,000
	MAQC B	3	polyA-enriched	199	5,743,028	1,140
	ERCC 1	1	polyA-enriched	206	6,835,287	1,410
	ERCC 2	2	polyA-enriched	207	7,119,023	1,480
	ERCC 1	1	polyA-enriched	182	6,525,478	1,190
	ERCC 2	1	polyA-enriched	191	5,490,495	1,050
4(S) Proton	MAQC A	3	polyA-enriched	78	50,063,784	3,900
	MAQC B	3	polyA-enriched	85	53,203,028	4,497
5(B) Proton	MAQC A	1	polyA-enriched	95	57,701,947	4,864
	MAQC B	1	polyA-enriched	75	39,099,605	2,946
	MAQC C	1	polyA-enriched	64	41,308,206	6412,641
	MAQC D	1	polyA-enriched	53	46,665,851	3,160
6(L) Proton	MAQC A	1	polyA-enriched	99	60,106,614	5,978
	MAQC B	1	polyA-enriched	100	60,769,231	6,085
	MAQC C	1	polyA-enriched	107	60,353,696	6,454
	MAQC D	1	polyA-enriched	106	69,977,984	7,413

---

**Pacific Biosciences RS**


---

Labs	Samples	Libraries per Sample: Size Fractionation	Preparation <sup>8</sup>	Avg. Read Length	Reads/Mb	Output (Mb)
1(A)	MAQC A	1: >3 kb	polyA + 5'G cap	3,983	251	663
	MAQC A	1: 2-3 kb	polyA + 5'G cap	3,513	284	520
	MAQC A	1: 1-2 kb	polyA + 5'G cap	2,811	356	780
	MAQC B	1: >3 kb	polyA + 5'G cap	3,467	288	536
	MAQC B	1: 2-3 kb	polyA + 5'G cap	3,223	310	459
	MAQC B	1: 1-2 kb	polyA + 5'G cap	3,112	321	638
2(F)	MAQC A	1: >3 kb	polyA + 5'G cap	3,472	288	634
	MAQC A	1: 2-3 kb	polyA + 5'G cap	3,644	274	555
	MAQC A	1: 1-2 kb	polyA + 5'G cap	2,792	358	927
	MAQC A	1: unfractionated	polyA + 5'G cap	2,832	353	260
	MAQC B	1: >3 kb	polyA + 5'G cap	3,578	280	667
	MAQC B	1: 2-3 kb	polyA + 5'G cap	3,523	284	594

Pacific Biosciences RS						
Labs	Samples	Libraries per Sample: Size Fractionation	Preparation <sup>8</sup>	Avg. Read Length	Reads/Mb	Output (Mb)
	MAQC B	1: 1-2 kb	polyA + 5'G cap	2,844	351	991
	MAQC B	1: unfractionated	polyA + 5'G cap	2,814	355	251
	MAQC A	1: >3 kb	polyA + 5'G cap	3,201	312	528
	MAQC A	1: 2-3 kb	polyA + 5'G cap	3,135	319	344
	MAQC A	1: 1-2 kb	polyA + 5'G cap	2,761	362	767
3(H)	MAQC A	1: unfractionated	polyA + 5'G cap	2,998	334	477
	MAQC B	1: >3 kb	polyA + 5'G cap	3,189	314	572
	MAQC B	1: 2-3 kb	polyA + 5'G cap	2,952	339	383
	MAQC B	1: 1-2 kb	polyA + 5'G cap	2,779	360	660
	MAQC B	1: unfractionated	polyA + 5'G cap	3,069	326	395
Roche 454 FLX						
Labs	Samples	Libraries per Sample	Preparation <sup>9</sup>	Median Read Length	Total Reads per PicoTiterPlate	Output (Mb)
	MAQC A	1	polyA-enriched	520	1,061,320	552
1(I)	MAQC B	1	polyA-enriched	494	1,001,678	495
	MAQC A	1	polyA-enriched	497	805,399	400
	MAQC B	1	polyA-enriched	496	1,076,634	534
2(P)	MAQC A	1	polyA-enriched	455	832,580	379
	MAQC B	1	polyA-enriched	470	1,181,610	555
3(C)	MAQC A	2	polyA-enriched	505	1,294,497	654
	MAQC B	2	polyA-enriched	358	293,471	105

<sup>1</sup> Illumina RNA TruSeq v2 library kit,

<sup>2</sup> Illumina RNA TruSeq v3 library kit,

<sup>3</sup> RNaseA degraded,

<sup>4</sup> heat degraded,

<sup>5</sup> sonicated

<sup>6</sup> ERCC: synthetic standards only (External RNA Control Consortium); VL: pilot data for sample A or B;

<sup>7</sup> Ion Total RNA-Seq v2 library kit

<sup>8</sup> PacBio Large Insert Template Prep Kit

<sup>9</sup> Roche cDNA Rapid Library kit